Materials & Design 224 (2022) 111274

Contents lists available at ScienceDirect

Materials & Design

journal homepage: www.elsevier.com/locate/matdes

Powder injection molded ceramic scaffolds: The role of pores size and surface functionalization on the cytocompatibility

Martina Martínková [a,*], Berenika Hausnerová [a,b], Jakub Huba [b], Tomáš Martínek [c], Simona Káčerová [a], Věra Kašpárková [a,b], Petr Humpolíček [a,b,*]

[a] Tomas Bata University in Zlin, Centre of Polymer Systems, tr. Tomase Bati 5678, Zlin 76001, Czech Republic
[b] Tomas Bata University in Zlin, Faculty of Technology, Vavreckova, 275, Zlin 76001, Czech Republic
[c] Tomas Bata University in Zlin, Faculty of Applied Informatics, Nad Stranemi, 4511, Zlin 76005, Czech Republic

GRAPHICAL ABSTRACT

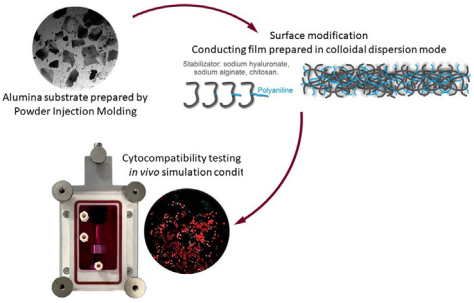

ARTICLE INFO

Article history:
Received 6 April 2022
Revised 5 October 2022
Accepted 19 October 2022
Available online 20 October 2022

Keywords:
Powder Injection Molding
Surface Modification
Polyaniline
Alumina
Tissue Engineering
Cytocompatibility

ABSTRACT

The alumina-based scaffolds prepared by powder injection molding can be preferentially used for preparation of bone grafts. Here, the final architecture of alumina scaffolds was efficiently controlled by powder space holder size and volume ratio. The alumina is not intrinsically cell-instructive material and thus the coating with electrically-conducting polyaniline or polyaniline/biopolymer films prepared in a colloidal dispersion mode was used to provide this advanced property. The component of the extracellular matrix, sodium hyaluronate, or natural biopolymers (sodium alginate or chitosan) were employed, and, subsequently, the cytocompatibility of the native and functionalized alumina scaffolds were determined. Both the absence of cytotoxicity and the cytocompatibility that were revealed demonstrate the application potential of these composites. The scaffolds with pore size greater than 250 μm were more cytocompatibility than those with pores size between 125 and 250 μm. The cytocompatibility was confirmed under *in vivo*-mimicking dynamic cultivation conditions which further improve the cell distribution and growth.

1. Introduction

Personalized medical devices such as dental prostheses, bone grafts or personalised medical devices often require the preparation of precisely designed scaffolds. While 3D printing techniques are applicable for polymer-based scaffolds, Powder Injection Molding (PIM) allows the preparation of precisely designed ceramics-

Abbreviations: CBS, ceramic-based scaffold; CH, chitosan; SA, sodium alginate; SH, sodium hyaluronate; AH, aniline hydrochloride; APS, ammonium persulfate.

* Corresponding authors.
E-mail addresses: martinkova@utb.cz (M. Martínková), hausnerova@utb.cz (B. Hausnerová), jhuba@utb.cz (J. Huba), tmartinek@utb.cz (T. Martínek), s_kacerova@utb.cz (S. Káčerová), vkasparova@utb.cz (V. Kašpárková), humpolicek@utb.cz (P. Humpolíček).

https://doi.org/10.1016/j.matdes.2022.111274
0264-1275/

based products made. The precise design together with homogeneous chemical composition [1] is considered as main advantages of PIM made materials. PIM allow to fabricate the personalised medical devices made of ceramics which can be especially advantageous in bone or dental engineering. The resulting porous PIM structures have a different internal structure to those fabricated by additive manufacturing plus allows to control the porosity [2].

Aluminum oxide (alumina) has good biocompatibility [3], excellent corrosion resistance, high wear resistance and strength, and is chemically bioinert [4]. In addition, its price is substantially lower in comparison to, for example, titanium alloys. It should also be mentioned that the production of porous alumina structures is not as demanding as in the case of titanium and its alloys, which are highly reactive and thus must be mixed, molded, and also debound/sintered carefully under protective atmospheres.

Both, the bulk and surface properties must be considered when the cytocompatibility of scaffolds are considered. From the bulk properties, the pore shape is known to affect cell behavior, as in the bone tissue regeneration process, the size and interconnection of pores affect the cell migration, proliferation, and ingrowth into the scaffold [5]. Another bulk properties such porosity [6], thermal conductivity [7], and elasticity [8] is not limited the ceramic-based scaffolds (CBS) application, but the surface characteristics are. Thus, the composites combining the appropriate bulk characteristics with stimuli-responsive surface coatings seems to be the most appropriate way for preparation of desired cell-instructive scaffolds.

One of the most suitable materials for the preparation of stimuli-responsive, and thus cell-instructive coatings is polyaniline (PANI) [5]. PANI is a widely studied conducting polymer that possesses some unique properties. For example, the coating by PANI itself is not adequately cytocompatible, but can be combined with a variety of biomolecules, by the preparation of thin films based on colloidal dispersions, to produce cytocompatible films [9,10]. PANI also intrinsically combines electronic and ionic conductivities, which is advantageous for material/cell communication. As mentioned, PANI can be stabilized by biopolymers that influence the cellular physiology [11,12]. The following compounds can be used as stabilizers: sodium hyaluronate, which can provide final material-specific bioactivity, especially changes in stem cell gene expression [13]; chitosan, which is well known for its antibacterial properties [14]; and alginate, which is widely used in a variety of biomedical applications including tissue engineering [15].

There have been studies devoted to the space-holder-assisted PIM of metal powders such as 316 L stainless steel and several titanium alloys, but there has hitherto been no report on aluminum oxide. Considering the shape of the pores, polymethyl methacrylate (PMMA) was used as a spherical space-holder for 316 L stainless steel [16,17] and Ti6Al4V [18], while sodium chloride (NaCl) and potassium chloride (KCl) have been employed in cases where an irregular shape of particles or fibers with a high L/D ratio is desired. Thus, one of the novelties of presented study is the use of KCl as space holder for aluminium oxide. Another innovative feature of the approach used in the present study is the colloidal-based coating of surfaces. Concretely, the surfaces of a substrate were coated with various films based on polyaniline (PANI) stabilized by biopolymers – in this case, sodium hyaluronate, chitosan, and sodium alginate. Using these biopolymers, cell compatibility, or more generally the biocompatibility of materials, might be controlled.

2. Materials and methods

2.1. Preparation of native ceramic-based substrates

The powder components of the PIM compound were aluminum oxide (Martinswerk – Huber Corporation, USA) (ρ = 3.98 g/cm^3, size range 0.1–3.0 μm) and a powder space holder (PSH), potassium chloride (KCl, Sigma Aldrich, Germany) (ρ = 1.98 g/cm^3, size range 125–500 μm). The powders were admixed into a partially water-soluble binder (Licomont EK 583, ρ = 1.08 g/cm^3, viscosity 1.5 mPa.s at 130 °C) in a batch mixer (Plasti-Corder, Brabender, Germany) with counter-rotating blades. The powder content was kept at 60 vol%, the powder: PSH ratio varied from 20:40 to 50:10, and two size ranges of the PSH were tested, see Table 1 (samples marked as CBS – Ceramic Based Substrates).

Injection molding was performed on an injection molding machine (Allrounder 370S, Arburg, ARBURG GmbH + Co KG, Lössburg, Germany) with a universal tooling frame. The inserts for test samples were made by machining EN AW 7022 aluminum alloy. The test geometry consisted of a round plate (diameter 45 mm) with a highly-drafted angle due to the absence of an ejector system. The molding pressures were optimized to obtain defect-free samples, (see Table 1).

Afterwards, the water-soluble binder component and part of the PSH were removed by immersion in distilled water (60 °C) for 24 h. The remaining binder (the backbone) was debound thermally (280 °C) at atmospheric pressure. Sintering was carried out in a PIM furnace (CLASIC CZ s.r.o., Revnice, Czech Republic) up to a maximum temperature of 1670 °C and for a holding time of 1 h. The surface of CBS were inspected using SEM microscopy (VEGA, Tescan).

2.2. Surface functionalization of native substrate

The surface of native CBS was further coated to become bioactive. Four different compositions of the coating were tested. Firstly, polyaniline (PANI) was used for coating. This coating can provide electroactivity but according to previous studies does not provide adequate cytocompatibility. Another three coatings were therefore prepared *via* the innovative *in-situ* polymerization of aniline hydrochloride in the presence of stabilizers – concretely, sodium hyaluronate (SH), sodium alginate (SA), and chitosan (CH) [11]. The final composite coating is denominated either as PANI/SH, PANI/SA, or PANI/CH. In all cases, aniline hydrochloride (AH, Sigma Aldrich, Germany) and ammonium persulfate (APS, Sigma Aldrich, Germany) were used for the preparation of each coating.

Preparation of PANI coating. PANI films were prepared by mixing 0.2 M AH and 0.25 M APS solutions and then pouring the reaction mixture over samples and into Petri dishes. After 1 h of polymerization, the surfaces were washed with 0.2 M HCl (Penta, Czech Republic) and rinsed with methanol (Penta, Czech Republic).

Preparation of PANI/SH coating. For the preparation of PANI with SH, 0.2 M AH, 0.1 M APS, and 1 % SH (Contipro a.s., Czech Republic) were used. SH in demineralized water was shaken at 55 °C overnight. Then, the AH solution was added, followed by the APS solution. The reaction mixture was poured over samples and into Petri dishes, and polymerization carried out for 4 h.. As before, this step was followed by washing with 0.2 M HCl and rinsing with methanol.

Preparation of PANI/SA coating. PANI film stabilized with sodium alginate (IPL, Czech Republic) was prepared using 0.2 M AH, 0.25 M APS, and 2 % SA. The solution of SA was made in demineralized water and shaken at 37 °C overnight. Afterward, AH was added, followed by APS; thereafter, samples and the Petri dishes were coated with the PANI/SA mixture. The polymer films were allowed to polymerize for 4 h. The last step was the fixation of films with 0.2 M HCl and methanol.

Preparation of PANI/CH coating. This surface modification was made with 0.2 M AH, 0.01 M APS, and 2 % chitosan (Sigma Aldrich, Germany). Firstly, a solution of CH was prepared by dissolving it in 1 M HCl and shaking the solution at 55 °C overnight. After filtration of the solution, AH was added, followed by APS. The surfaces were

Table 1
Composition of mixture and parameters of powder injection moulding process. Two ranges of PSH grain sizes were used in this study, firstly grains in the size range of 125–250 ($^{\leq 250}$) μm and grains of 250–500 μm ($^{\geq 250}$).

Abbreviation	Powder Space Holder		Powder	Pressure [bar]	
	size [μm]	[vol.%]	[vol.%]	Injection	Holding
$CBS^{\geq 250\_A}$	250–500	20	40	2100	1650
$CBS^{\geq 250\_B}$		30	30	1500	1200
$CBS^{\geq 250\_C}$		40	20	1900	1500
$CBS^{\geq 250\_D}$		50	10	2100	1650
$CBS^{\leq 250\text{-}E}$	125–250	20	40	2100	1650
$CBS^{\leq 250\text{-}F}$		30	30	1500	1200
$CBS^{\leq 250\text{-}G}$		40	20	1900	1500
$CBS^{\leq 250\text{-}H}$		50	10	2100	1650

covered with the resulting mixture and the film was left to polymerize for 12 h. Subsequently, the films were washed with 0.2 M HCl and rinsed with methanol.

2.3. Cytotoxicity determination

In the tests, a mouse embryonic fibroblast cell line (ATCC CRL-1658 NIH/3T3, USA) was used. The cultivation medium consisted of Dulbecco's Modified Eagle's Medium (PAA Laboratories GmbH, Austria) containing 10 % bovine calf serum (BioSera, France) and 1 % of Penicillin/Streptomycin (GE Healthcare HyClone, United Kingdom). The test was repeated twice, each with five repetitions per sample. Cells were incubated at 37 °C in 5 % CO_2 in humidified air.

Cytotoxicity of the native substrate. Native CBS were crushed and extracted according to ISO standard 10993–12 in media with a concentration of 0.2 g/mL. The tested samples were extracted in a culture medium for 24 h at 37 °C with stirring. The parent extracts (100 vol%) were then diluted in the culture medium to achieve final concentrations of 75, 50, 25, 10, and 1 vol%. All extracts were used within 24 h.

Cytotoxicity testing itself was performed according to ISO protocol 10 993–5. Cells were preincubated in 96 well plates (TPP, Switzerland) at a concentration of 10^5 cells per mL. The extracts were added to pre-cultivated cells for another 24 h. All tests were performed in quadruplicates. The evaluation of cell viability at the end of exposure was performed using Tetrazolium (MTT cell proliferation assay kit, Duchefa Biochemie, Netherlands). The absorbance was measured at 570 nm with an Infinite M200 Pro NanoQuant instrument (Tecan, Switzerland) and the reference wavelength was adjusted to 690 nm. The results are presented as the cell viability (%) in NIH/3T3 culture compared to that in medium without PIM extracts (reference cell viability corresponds to 1). The morphology of cells from the culture plates was assessed after their cultivation in CBS extracts by using an inverted Olympus IX 81 phase contrast microscope (Olympus, Germany).

2.4. Cytocompatibility determination

The cytocompatibility study began with the determination of cell adhesion, growth, and proliferation on (1) native CBS and (2) the films used for its functionalization. The results from these initial steps allowed us to design and perform (3) bioactivity studies in which cell growth and ingrowth under static or dynamic conditions with electrical stimulation were investigated.

The cultivation conditions for experiments 1 and 2 were the same: the cells were incubated at 37 °C in humidified air with 5 % CO_2 for 2 days. The differences were in the concentrations of seeded cells: 2×10^5 per mL for experiment 1, and half that concentration (10^5 per mL) for experiment 2. The experimental setup and cultivation conditions for experiment 3 were adjusted as follows: A concentration of 2×10^5 cells per mL was seeded on substrates with a functionalized surface. After 3 days of proliferation, samples were transferred to a bioreactor enabling electrical stimulation. The bioreactor was run for 6 h per day for a total run-time of 72 h, each successive hour-long period alternating between electrical stimulation and no stimulation. The medium flow was 54 RPM. The pulse had a rectangular waveform with a width of 3000 ms, and the voltage was set at 0.1 V. Cells were visualised through nuclei counterstaining by Hoechst 33,258 (Invitrogen, USA) and actin filaments were visualized by counterstaining with ActinRed™ 555 (Thermo Fisher Scientific, USA).

3. Results and discussion

3.1. Space holder size and volume determine the architecture of CBS

Substrate composition, architecture, pore size, and porosity all play important roles in the context of designing materials for use within biomedicine. Here, we used different sizes of space holder, different space holder *vs* powder ratios, and different processing parameters. Scaffold porosity increases with increasing additions of the powder space holder. In addition, the shape of the pores can be influenced by the shape of the PSH grains. As can be clearly seen in Fig. 1, the critical parameter determining the material properties is the space holder size and its ratio to powder, while processing parameters seems to be less important. Using these two components, the architecture, porosity, and especially the pore size can be easily controlled.

3.2. Native CBS do not induce cytotoxicity

The level of cytotoxicity predetermines any application of a material in biomedicine. Here, the ISO procedure was used to determine the cytotoxicity of the native substrate. The cytotoxicity evaluation is based on the determination of effect of soluble impurities leaching from the material, thus the cytotoxicity of substrates with functionalized surfaces was not determined, as the volume ratio of coatings was very low and could not thus induce cytotoxicity. The surface functionalization can however influence the cytocompatibility due to receptor-based interaction with cells. This issue is determined and discussed further.

As presented in Fig. 2, the native CBS did not induce cytotoxicity. Only in the case of two samples, $CBS^{\geq 250\_B,}$ $CBS^{\leq 250\text{-}F}$ marked as B and F, the cell viability slightly decreased bellow the 70 %, and thus approach the cytotoxicity threshold. If the standard deviations and cytotoxicity of higher concentrations (in case of sample B) are considered, the cytotoxicity of those concentrations was not clearly proved. It can thus be concluded that native CBS are applicable in biomedicine and can be further functionalized to become bioactive.

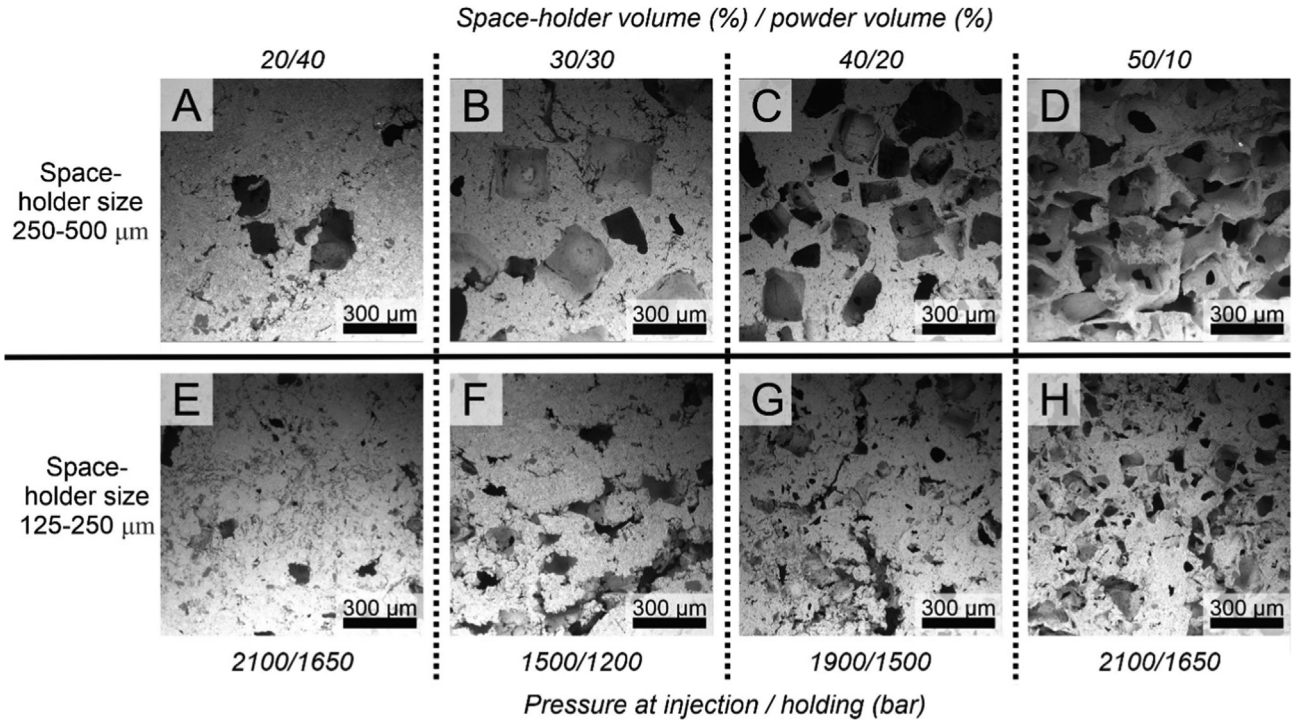

Fig. 1. SEM images of the structure of native CBS prepared using different compositions and preparation parameters. The effect of the size of the space-holder as well as the ratio between space and powder volume on the final structure of the substrate can be clearly seen. The pore size is highly correlated to the size of space holder, while the space holder / powder volume ration predetermine the porosity and pore interconnection. A = $CBS^{\geq 250\_A}$ B = $CBS^{\geq 250\_B}$, C = $CBS^{\geq 250\_C}$, D = $CBS^{\geq 250\_D}$, E = $CBS^{\leq 250\text{-}E}$, F = $CBS^{\leq 250\text{-}F}$, G = $CBS^{\leq 250\text{-}G}$, H = $CBS^{\leq 250\text{-}H.}$

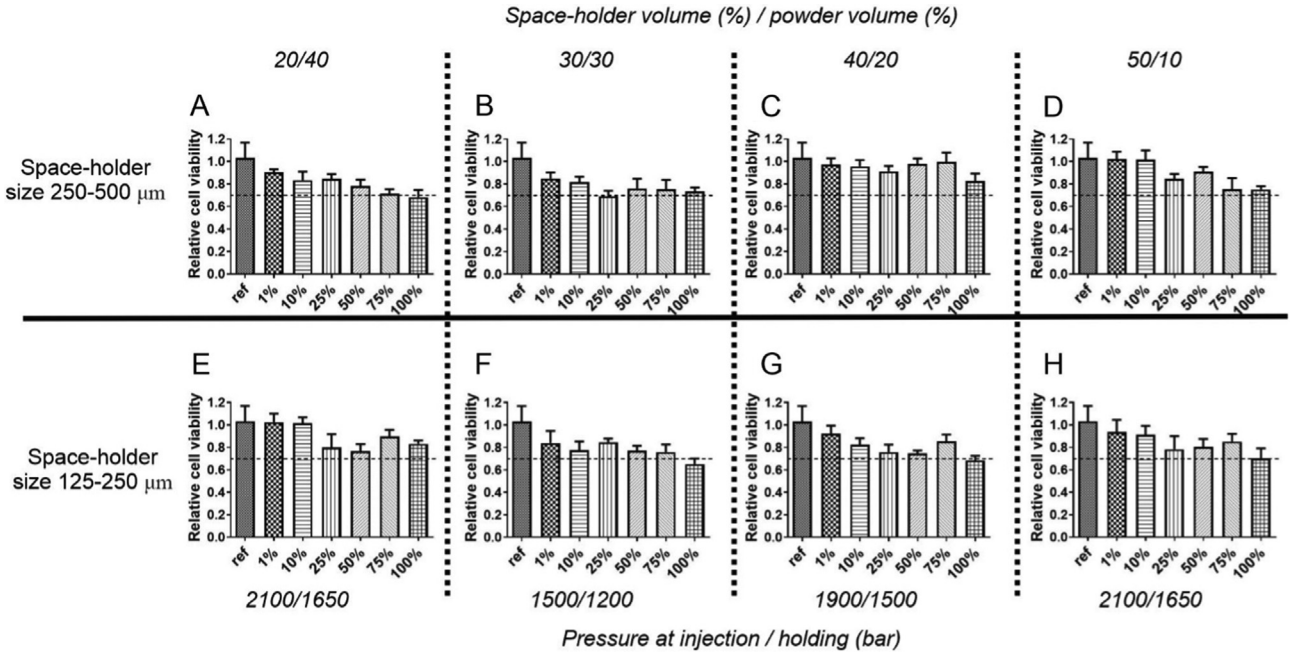

Fig. 2. The cytotoxicity of native CBS determined by a decrease in cell viability compared to the reference (data were converted to a percentage of the control and expressed as the mean ± standard deviation, n = 5). The ISO 10–993 procedure, concretely the testing of extracts, was used. The cytotoxicity threshold is marked by dashed lines; when the viability falls below 70 %, samples are considered to induce cytotoxicity. None of the tested native substrates induced cytotoxicity. A = $CBS^{\geq 250\_A}$; B = $CBS^{\geq 250\_B}$, C = $CBS^{\geq 250\_C}$, D = $CBS^{\geq 250\_D}$, E = $CBS^{\leq 250\text{-}E}$, F = $CBS^{\leq 250\text{-}F}$, G = $CBS^{\leq 250\text{-}G}$, H = $CBS^{\leq 250\text{-}H.}$

3.3. Bioactive coatings prepared in colloidal dispersion mode are cytocompatible

The conductivity is one of the crucial properties when the bioactivity of bone scaffolds and grafts are considered [19]. The conductivity can be achieved by incorporation of conducting polymers. It was, however, previously determined that native PANI does not provide an adequate cell response, which was also confirmed by this study (see Fig. 3B). Functionalization was therefore performed by means of an innovative procedure combining the

synthetic conducting polymer (providing stimuli-responsivity) with biopolymers (providing cytocompatibility). The procedure is based on the preparation of thin films in colloidal dispersion mode [10]. The final composite coating can thus provide both bioactivity and cytocompatibility.

To confirm the cytocompatibility of the surface functionalization employed here, cells were seeded onto surfaces and their proliferation and morphology were determined. The quantification of cells on the individual surfaces was not determined due to both the interaction of films with reagents used for cell viability evaluation (especially the MTT assay results can be biased) and due to the fact, that cell quantity does not provide relevant information about the real cytocompatibility which depends on cell physiology and morphology. It is clearly shown that cells on the PANI films were not capable of proliferation (see Fig. 3B). From the study [11], it is known that the addition of biocompatible polysaccharides to colloidal films changes the surface energy and surface topography, which can also lead to a change in cytocompatibility. Fig. 3C show that the number of cells on the surface modified with PANI/SA was smaller than the numbers of cells on the surfaces modified with PANI/SH (Fig. 3E) and PANI/CH (Fig. 3D) film. Also, on PANI/SA (Fig. 3C), round cells could be observed that were capable of adhering onto the surface, but they could not proliferate. The number of cells on the surface stabilized by alginate was smaller in comparison to the other stabilized films. Fig. 3E shows the cell on the surface coated with PANI/SH are present in higher quantity and especially their morphology is more physiological. This could be because of SH, which can support not only cell adhesion and proliferation but mainly their physiological state according to the type of adhered cells. The actin cytoskeleton of cells on this film was more fibrous compared to the reference sample (Fig. 3A). The proliferation rate on the PANI/CH film (Fig. 3D) was similar to that on the PANI/SH film and also the morphology of actin fibers was similar in these two cases. It can be clearly seen that the best cytocompatibility was offered by the PANI/SH and PANI/CH coatings. From those, the PANI/SH was later chosen as the most promising treatment for the determination of bioactivity under dynamic cultivation conditions. Sodium hyaluronate was chosen with regard to bioactivity related to stem cell differentiation [20].

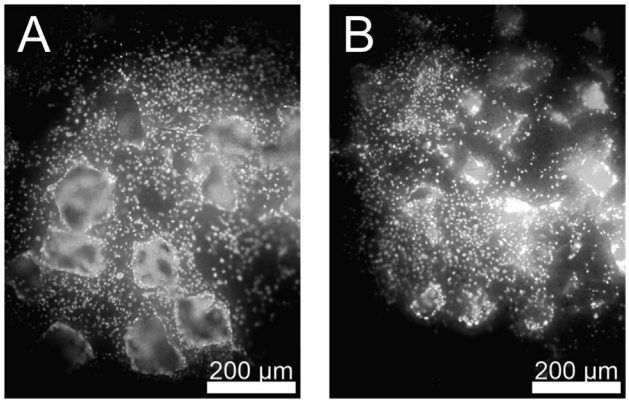

Fig. 4. Cell growth on the surface and within the pores of native $CBS^{\geq 250\_B}$ (A) and $CBS^{\leq 250\_F}$ (B) prepared with 30 vol% of space holder. The cells were seeded in a concentration of 2×10^5 cells per mL and cultivated for 2 days. Individual cells were visualised through nuclei counterstaining by Hoechst (white). There were no significant differences between any of native CBS. The $CBS^{\geq 250\_D}$ were chosen as the most appropriate for other experiments.

3.4. Cells can grow on the surface and within the pores of CBS under static cultivation conditions

In addition, cell growth on the surface of the sample, as well as cell ingrowth into the pores were investigated on native as well functionalized CBS. Cells were able to attach to, and subsequently grow on all mentioned samples.

Fig. 4 provides a detailed view of the surface of the native CBS without any surface treatment and with different pores sizes (A 250 μm and more, B 125–250 μm). Overall, the growth of cells was better on samples with a pore size greater than 250 μm than on samples with a pore size between 125 and 250 μm. The lowest viability was observed for CBS functionalized with PANI. In contrast, functionalization by films prepared in colloidal dispersion mode improved cell growth on PIM samples in the case of all stabilizers. Also, there were no significant differences in cell growth between $CBS^{PANI/SH}$, $CBSP^{PANI/SA}$, and $CBS^{PANI/CH}$. Moreover, the cell

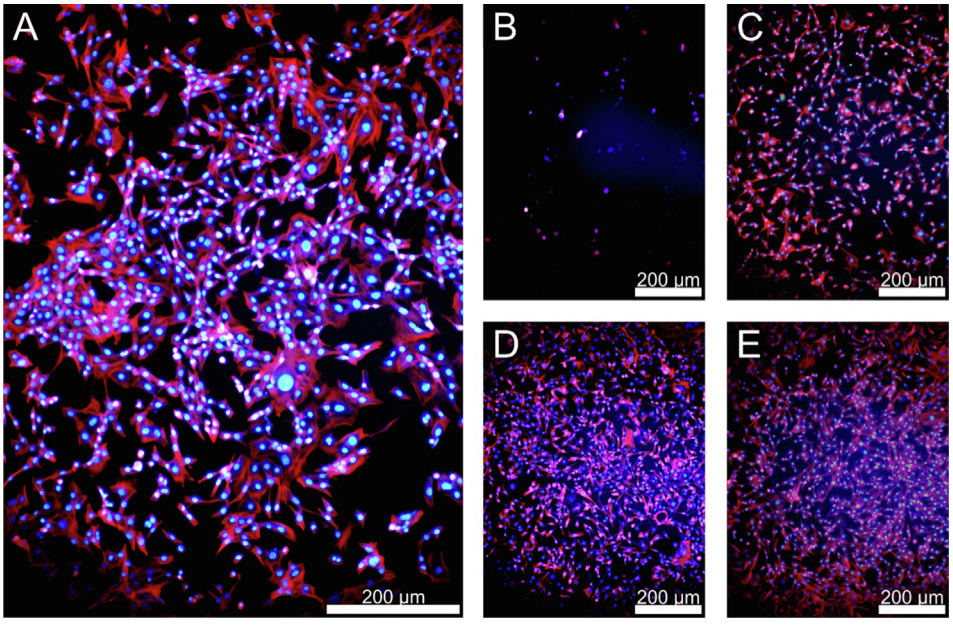

Fig. 3. Cell proliferation on reference – the cell culture polystyrene without surface modification (A); PANI (B), PANI/SA (C); PANI/CH (D); and PANI/SH (E). Cells were seeded in a concentration of 10^5 cells per mL and cultivated for 2 days. Cell nuclei were visualized by counterstaining with Hoechst; actin filaments were visualized by counterstaining with ActinRed™ 555 The appropriate cytocompatibility was observed in the case of the PANI/CH and PANI/SH coating.

quantity was very similar to that observed for pure PIM samples. Based on microscopic observations it can be concluded, that cells were able to ingrowth deeper into the pores in all of the samples.

Due to the best cytocompatibility of CBS with pores higher than 250 μm and most promising properties of PANI/SH based coating the only CBS$^{\geq 250_D_PANI/SH}$ was used for further experiments.

3.5. Dynamic conditions and electrical stimulation improve cytocompatibility

The final goal of the here presented study was to prepare a CBS which is not only cytocompatible but also possess stimuli-responsive and thus even cell-instructive potential. The importance of *in vivo* occurred dynamic condition is often omitted within the cytocompatibility study. In this context, the mechanotransduction which integrates various physical cues from a cell's surrounding microenvironment and converts them into biochemical intracellular signaling responses are most important. The flow of cultivation medium (shear stress) is main part of mechanotransduction when the bone scaffolds are considered. Here we apply the media flow 54 RPMI. Except of mechanotransduction, the instructive role of electroconductivity is obviously of great importance. Especially in case of bone tissue, the role of electroconductivity of materials is discussed [21].

There are no generally accepted protocols used for the electrical stimulation of cells, the set-ups vary not only in the applied voltage (from ~ 4–5 mV to 150 mV) but also pulse duration (mostly from 2 ms to 200 ms), frequency (mostly between 2 and 6 Hz), and waveform (e.g. monophasic, square) [19,22,23]. In here presented experiments the commercial equipment was used and the electrical stimulation parameters were as follows: voltage 0.1 V, pulse width 3000 ms, arrangement on square-wave.

As mentioned, the CBS with a pore size above 250 μm was chosen for the experiments under dynamic conditions. The preferential cytocompatibility of materials with pore size of about 200 to 300 μm is generally considered as ideal for bone tissue replacements [24] and was confirmed even on the CBS (see Fig. 4A). The coating with PANI/SH was chosen as the most promising, mainly due to the bioactivity of SH.

Both described cell-stimuli external factors, shear stress and external electrical stimuli, were applied together, and the results are presented in Fig. 5. It is obvious that application of shear stress and external electrical stimulation has an important effect on few cellular parameters (please compare the Fig. 5A and 5B versus 5C and 5D). Firstly, the cell quantity is higher on the surfaces exposed to dynamic conditions, and more importantly the cell distribution is more homogeneous. This is critical for the scaffold acceptance after implantation [25]. In addition, a slightly different cell morphology and structure of cytoskeleton can be observed under dynamic conditions with electrical pulses than under static conditions. This can be connected to both the applied shear stress and electrostimulation [26,27].

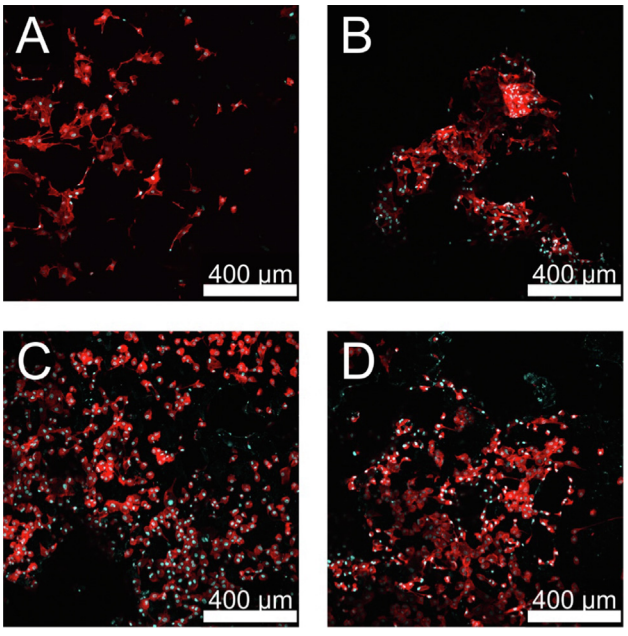

Fig. 5. Cell distribution and cell morphology on CBS$^{\geq 250_D_PANI/SH}$ under static (A,B) or dynamic (C,D) cultivation conditions. Cells were seeded in a concentration of 2 × 10^5 cells per mL and precultivated in static conditions for 3 days and subsequently cultivated in dynamic conditions for another 3 days. Cell nuclei are visualized by counterstaining with Hoechst, actin filaments are visualized by counterstaining with ActinRed. Parameters of dynamic conditions: Media flow 54 RPMI, pulse width 3000 ms, square waveform, voltage 0.1 V.

4. Conclusion

Ceramic-based scaffolds prepared by Powder Injection Molding are promising candidates for use as medical scaffolds, especially in bone regeneration and restoration. The composition of the PIM mixture as well as the processing parameters were tested to reveal their impact on the architecture of the porous material. It was found that the final architecture can be efficiently controlled by the powder space holder size and the volume ratio. However, alumina itself does not provide adequate cytocompatibility, or, especially, bioactivity. None of the prepared ceramic-based scaffolds induced cytotoxicity, and more importantly, cells were able to grow on their surface and ingrowth into the pores. The scaffolds surfaces were therefore subsequently functionalized by stimuli-responsive polyaniline-based films. To improve the cytocompatibility, coatings were innovatively prepared in colloidal dispersion mode and combined the synthetic conducting polymer with biopolymer stabilizers (sodium hyaluronate, chitosan, and sodium alginate). This functionalization further significantly improved the cytocompatibility of the ceramic-based scaffolds. The bioactivity of the prepared scaffolds was confirmed by an improvement in cytocompatibility when dynamic cultivation conditions and electrical impulses were applied. The *in vivo* mimicking conditions improve the cytocompatibility of scaffolds, especially in context of cell distribution and growth.

Data availability

Data will be made available on request.

Declaration of Competing Interest

The authors declare that they have no known competing financial interests or personal relationships that could have appeared to influence the work reported in this paper.

Acknowledgements

The work was supported within the project OP RDE Junior Grants of TBU in Zlin, Reg. No. CZ.02.2.69/0.0/0.0/19_073/0016941 (JUNG-2020-001), Czech Science Foundation (20-28732S) and Ministry of Education, Youth and Sports of the Czech Republic – DKRVO (RP/CPS/2022/001 and RP/CPS/2022/003).

Appendix A. Supplementary material

Supplementary data to this article can be found online at https://doi.org/10.1016/j.matdes.2022.111274.

References

[1] G. Matula, A. Szatkowska, K. Matus, B. Tomiczek, M. Pawlyta, Structure and properties of Co-Cr-Mo alloy manufactured by powder injection molding method, Materials 14 (8) (Apr. 2021) 2010, https://doi.org/10.3390/ma14082010.

[2] D. Zhao et al., Surface topography and cytocompatibility of metal injection molded Ti–22Nb alloy as biomaterial, Trans. Nonferrous Metals Soc. China 28 (7) (Jul. 2018) 1342–1350, https://doi.org/10.1016/S1003-6326(18)64772-7.

[3] M. Rahmati, M. Mozafari, Biocompatibility of alumina-based biomaterials–a review, J. Cell Physiol. 234 (4) (Apr. 2019) 3321–3335, https://doi.org/10.1002/jcp.27292.

[4] D.F. Heaney, J.D. Gurosik, C. Binet, Isotropic forming of porous structures via metal injection molding, J. Mater. Sci. 40 (4) (Feb. 2005) 973–981, https://doi.org/10.1007/s10853-005-6516-1.

[5] Y. Arteshi, A. Aghanejad, S. Davaran, Y. Omidi, Biocompatible and electroconductive polyaniline-based biomaterials for electrical stimulation, Eur. Polym. J. 108 (Nov. 2018) 150–170, https://doi.org/10.1016/j.eurpolymj.2018.08.036.

[6] J.L. Hernandez, K.A. Woodrow, Medical Applications of Porous Biomaterials: Features of Porosity and Tissue-Specific Implications for Biocompatibility, Adv Healthcare Materials 11 (9) (May 2022) 2102087, https://doi.org/10.1002/adhm.202102087.

[7] M.S. Zafar et al., "Properties of dental biomaterials", in *Advanced Dental Biomaterials*, Elsevier (2019) 7–35, https://doi.org/10.1016/B978-0-08-102476-8.00002-5.

[8] A.M.J. Coenen, K.V. Bernaerts, J.A.W. Harings, S. Jockenhoevel, S. Ghazanfari, Elastic materials for tissue engineering applications: Natural, synthetic, and hybrid polymers, Acta. Biomater. 79 (Oct. 2018) 60–82, https://doi.org/10.1016/j.actbio.2018.08.027.

[9] P. Bober, P. Humpolíček, J. Pacherník, J. Stejskal, T. Lindfors, Conducting polyaniline based cell culture substrate for embryonic stem cells and embryoid bodies, RSC Adv. 5 (62) (2015) 50328–50335, https://doi.org/10.1039/C5RA07504A.

[10] V. Kašpárková et al., Cell-compatible conducting polyaniline films prepared in colloidal dispersion mode, Colloids Surf., B 157 (Sep. 2017) 309–316, https://doi.org/10.1016/j.colsurfb.2017.05.066.

[11] D. Jasenská et al., Conducting composite films based on chitosan or sodium hyaluronate. Properties and cytocompatibility with human induced pluripotent stem cells, Carbohydr. Polym. 253 (Feb. 2021), https://doi.org/10.1016/j.carbpol.2020.117244 117244.

[12] V. Kašpárková et al., Polyaniline colloids stabilized with bioactive polysaccharides: Non-cytotoxic antibacterial materials, Carbohydr. Polym. 219 (Sep. 2019) 423–430, https://doi.org/10.1016/j.carbpol.2019.05.038.

[13] M. Hemshekhar, R.M. Thushara, S. Chandranayaka, L.S. Sherman, K. Kemparaju, K.S. Girish, Emerging roles of hyaluronic acid bioscaffolds in tissue engineering and regenerative medicine, Int. J. Biol. Macromol. 86 (May 2016) 917–928, https://doi.org/10.1016/j.ijbiomac.2016.02.032.

[14] F. Croisier, C. Jérôme, Chitosan-based biomaterials for tissue engineering, Eur. Polym. J. 49 (4) (Apr. 2013) 780–792, https://doi.org/10.1016/j.eurpolymj.2012.12.009.

[15] J. Sun, H. Tan, Alginate-Based Biomaterials for Regenerative Medicine Applications, Materials 6 (4) (Mar. 2013) 1285–1309, https://doi.org/10.3390/ma6041285.

[16] H.Ö. Gülsoy, R.M. German, Production of micro-porous austenitic stainless steel by powder injection molding, Scr. Mater. 58 (4) (Feb. 2008) 295–298, https://doi.org/10.1016/j.scriptamat.2007.10.004.

[17] K. Nishiyabu, S. Matsuzaki, S. Tanaka, Net-Shape Manufacturing of Micro Porous Metal Components by Powder Injection Molding, MSF 534–536 (Jan. 2007) 981–984, https://doi.org/10.4028/www.scientific.net/MSF.534-536.981.

[18] G. Engin, B. Aydemir, H.Ö. Gülsoy, Injection molding of micro-porous titanium alloy with space holder technique, Rare Met. 30 (6) (Dec. 2011) 565–571, https://doi.org/10.1007/s12598-011-0430-2.

[19] L. Leppik et al., Combining electrical stimulation and tissue engineering to treat large bone defects in a rat model, Sci. Rep. 8 (1) (Dec. 2018) 6307, https://doi.org/10.1038/s41598-018-24892-0.

[20] M.B. Asparuhova, V. Chappuis, A. Stähli, D. Buser, A. Sculean, Role of hyaluronan in regulating self-renewal and osteogenic differentiation of mesenchymal stromal cells and pre-osteoblasts, Clin. Oral. Invest. 24 (11) (Nov. 2020) 3923–3937, https://doi.org/10.1007/s00784-020-03259-8.

[21] D.T. Dixon, C.T. Gomillion, Conductive Scaffolds for Bone Tissue Engineering: Current State and Future Outlook, JFB 13 (1) (Dec. 2021) 1, https://doi.org/10.3390/jfb13010001.

[22] K. Ronaldson-Bouchard et al., Advanced maturation of human cardiac tissue grown from pluripotent stem cells, Nature 556 (7700) (Apr. 2018) 239–243, https://doi.org/10.1038/s41586-018-0016-3.

[23] Z. Zhao et al., Optimization of Electrical Stimulation for Safe and Effective Guidance of Human Cells, Bioelectricity 2 (4) (Dec. 2020) 372–381, https://doi.org/10.1089/bioe.2020.0019.

[24] C.M. Murphy, M.G. Haugh, F.J. O'Brien, The effect of mean pore size on cell attachment, proliferation and migration in collagen–glycosaminoglycan scaffolds for bone tissue engineering, Biomaterials 31 (3) (Jan. 2010) 461–466, https://doi.org/10.1016/j.biomaterials.2009.09.063.

[25] C. Kleinhans et al., A perfusion bioreactor system efficiently generates cell-loaded bone substitute materials for addressing critical size bone defects, Biotechnol. J. 10 (11) (Sep. 2015) 1727–1738, https://doi.org/10.1002/biot.201400813.

[26] C. Chen, X. Bai, Y. Ding, I.-S. Lee, Electrical stimulation as a novel tool for regulating cell behavior in tissue engineering, Biomater. Res. 23 (1) (Dec. 2019) 25, https://doi.org/10.1186/s40824-019-0176-8.

[27] J. Hansmann, F. Groeber, A. Kahlig, C. Kleinhans, H. Walles, Bioreactors in tissue engineering-principles, applications and commercial constraints, Biotechnol. J. 8 (3) (Mar. 2013) 298–307, https://doi.org/10.1002/biot.201200162.